

Sign problems in path integral formulations of quantum mechanics and quantum statistics

Vladimir Filinov, Alexander Larkin¹

¹*Joint Institute for High Temperatures of the Russian Academy of Sciences,
Izhorskaya 13 Bldg 2, Moscow 125412, Russia*

Nowadays the term 'sign problem' is used to identify two different problems.

The ideas to overcome the first type of the 'sign problem' of strongly oscillating complex valued integrand in the Feynman path integrals comes from Picard-Lefschetz theory and a complex version of Morse theory. The main idea is to select Lefschetz thimbles as the cycle approaching the critical point at the path-integration, where the imaginary part of the complex action stays constant. Since the imaginary part of the action is constant on each thimble, the sign problem disappears and the integral can be calculated much more effectively. Here based on the Metropolis – Hastings algorithm a new method of calculations of the integral of the strongly oscillating integrands has been prosed. Some simple test calculation and comparison with available analytical results have been carried out.

The second type of the 'sign problem' arises at studies Fermi systems by path integral approach and is caused by the requirement of antisymmetrization of the real valued matrix elements of the density matrix. An explicit analytical expression for effective pair pseudopotential in phase space has been discussed in Wigner formulation of quantum mechanics. Obtained pseudopotential allow to account for Fermi statistical effects as realizes the Pauli blocking of fermions due to the repulsion between identical fermions, which prevents their occupation of same phase space cell. To test this approach, calculations of the momentum distribution function of the ideal system of Fermi particles have been presented over a wide range of momentum and degeneracy parameter.

PACS numbers: 03.65.- w, 05.10.Ln, 05.30.Fk, 2.38.Gc

Keywords: sign problems, path integrals, Lefschetz thimbles, Wigner functions

I. INTRODUCTION

One of the major difficulty for the Path Integral Monte Carlo (PIMC) simulation of the quantum systems of particles is so called 'sign problem'. The major aim of this paper is to discuss the new effective Monte Carlo methods for numerical simulations of path integrals with a sign problems as these methods can also provide a new perspectives in path integration. Our aim is to consider techniques of universal character, providing insights to this problems. However now a days the term 'sign problem' is used to identify two different problems.

The first type of the 'sign problem' arises in the Wigner and Feynman path integral formulation of quantum mechanics and the finite density quantum chromodynamics, where a complex action does not give a real and positive Boltzmann – like weight (for example, by the Wick rotation) to resort to the traditional Monte Carlo methods. The so-called reweighting algorithm is highly ineffective when the imaginary part of the action becomes very large, because one needs to take a sample from a configuration space, where the weights of nearby configurations have almost the same amplitudes but very different phases.

There has been many proposals to circumvent the 'sign problem'. Basic possible approach to this problem is to consider the variables, which are assumed to be real in the original formulation, to be complex and to extend the cycle of path-integration to a complex space in order to achieve better convergence.

So long under the typical physical conditions the integrand is holomorphic in the new complex variables and the final value of the path integral is unchanged by Cauchy's theorem. Making use of the Picard-Lefschetz theory and a complex version of Morse theory we can select the cycle approaching the saddle point at the path-integration, where the imaginary part of the complex action stays constant (Lefschetz thimbles) [1, 2]. Since the imaginary part of the action is constant on each thimble, the sign problem disappears and the integral can be calculated much more effectively.

However, since different thimbles are strongly separated, one needs to develop method to incorporate contributions from all relevant thimbles. To overcome this problem a natural choice is to use a gradient flow of action (described below), starting from the original real space of integration and creating a new manifold at a finite flow time, which is equivalent to the integration over original real space [3, 4]. In particular, when the flow time approaches infinity, the new manifold is composed of Lefschetz thimbles. In practise, as long as the finite flow-time is large enough then the 'sign problem' will be alleviated, as integral turn into integrals of an oscillating function with decaying amplitude. However reducing the amount of flow time may also reduce the effectiveness against the 'sign problem' and the multimodal problem simultaneously.

The alternative approach of sampling at calculation of the path-integrals on thimbles is based on the making use

of the complexified Langevin equation [5–7]. Of course, application of the noise leads to departures from the thimble, that accumulate and need to be corrected. Numerically, this procedure can be made stable.

Besides, the Langevin algorithm, other algorithms have been proposed: an Hybrid Monte Carlo algorithm [8], that however is essentially as expensive as the Langevin algorithm; two Metropolis algorithms [3, 9] that are simpler and faster, but have the risk of poor acceptance for large systems and an alternative algorithm [10] that ensures a control of the thimble at the price of limited scalability.

In this work we present the new Metropolis – Hastings algorithm for searching critical points and subsequent generation of the a Lefschetz thimbles. The algorithm allows to find critical points and to sample initial conditions for downward flows from the different quarters or halves of vicinity of the critical point. To increase efficiency of numerical procedure we have separated the Markovian transition on the complex plane in two sub-steps: the proposal and the acceptance-rejection. The proposal probability allow to propose a new state for given one. Here we are free in choosing proposing probability as it affect only the efficiency of the sampling the main contribution to the integrals and does not change the final result of calculations. The acceptance distribution is the conditional probability to accept/reject the proposed state.

The integrals involved in our test calculations are one variable integrals and can be performed analytically or independent numerically. However, it provides an interesting benchmark which can be seen as a limiting case of more realistic path integrals. It is non-trivial from the point of view of a Monte Carlo integration. For comparison with analytical results we present some calculations for the Airy function and some results on the Fourier transform of basic 1D factors comprising the Wiener path integral representation of the Wigner function in phase space. It also provides a case where different aspects of our approach can be clearly visualized.

The second type of the 'sign problem' arises from the requirement of antisymmetrization of the matrix elements of the fermion density matrix. As a result all thermodynamic quantities are presented as the sum of real valued terms with alternating sign related to even and odd permutations and are equal to the small difference of two large numbers, which are the sums of positive and negative terms. The numerical calculation in this case is severely hampered. To overcome this issue a lot of approaches have been developed but the 'sign problem' for strongly correlated fermions has not been fully solved during the last fifty years. Let us mention new original approaches developed in [11–15].

Monte Carlo simulations at finite temperature over the entire fermion densities range down to half the Fermi temperature have been carried out by permutation blocking path integral Monte Carlo (PB-PIMC) approach [12, 13]. For purpose to simulate fermions in the canonical ensemble, it was combined a fourth-order approximation of density matrix derived with a full antisymmetrization on all time slices in discrete versions of the paths. It was demonstrated that this approach effectively allows for the combination of $N!$ configurations from usual path integral MC into a single configuration weight of PB-PIMC, thereby reducing the complexity of the problem. Treatment of interacting fermions in [15] has been carried out at very high densities. Obtained results for finite number of particles were extrapolated to the thermodynamic limit [13].

The configuration path integral Monte Carlo (CPIMC) approach [14, 15] for degenerate correlated fermions with arbitrary pair interactions at finite temperatures is based on representation of the N -particle density operator in a basis of (anti-)symmetrized N -particle states (configurations of occupation numbers). The main idea of this approach is to evaluate the path integral in space of occupation numbers instead of configuration space. This leads to path integrals occupation number representation allowing to treat arbitrary pair interactions in a continuous space. However it turns out that CPIMC method exhibits a complementary behavior and works well at weak nonideality and strong degeneracy. Unfortunately, the physically most interesting region, where both fermionic exchange and interactions are strong simultaneously remains out of reach.

Another approach was proposed in [16], where to avoid the 'sign problem' and to realize Pauli blocking of fermions accounting for the Fermi statistical effects without antisymmetrization of the matrix elements the Wigner formulation of quantum mechanics in phase space has been used. In [16, 17] it has been shown that accounting for only the identical and pair permutations allow to derive an effective pair pseudopotential in phase space realizing the Pauli blocking. The derived repulsive pseudopotential depends on coordinates, momenta, and the degeneracy parameter of fermions and do not allow two identical fermions to occupy the same cell in phase cell. A new quantum phase space path integral Monte Carlo method has been also developed to calculate average values of arbitrary quantum operators in phase space. In this work we briefly present the basic ideas of this approach and test results for ideal degenerated fermions. Results for strongly interacting fermions in wide region of temperature and density for electron – hole plasma are presented in [11].

II. THE 'SIGN PROBLEM' OF THE COMPLEX VALUED INTEGRAND IN PATH INTEGRALS.

To explain the basic ideas we consider a one-dimensional quantum-mechanical system consisting of one particle in a potential field $U(q)$. The Hamilton function of such a system has the form:

$$H(p, q) = \frac{p^2}{2m} + U(q), \quad (1)$$

where p and q are the momentum and coordinate of the particle correspondingly. The potential function $U(q)$ is attractive and finite when q is real. Also we assume that the system is in a state of thermodynamic equilibrium with some external thermostat. In other words, we consider a canonical ensemble with temperature T and volume V (one-dimensional).

The quantum canonical ensemble can be fully characterized by the Wigner function $W(p, q)$, which is essentially a density matrix in the mixed coordinate-momentum representation and is defined as the Fourier transform of the density matrix in the coordinate representation:

$$W(p, q) = \int_{-\infty}^{+\infty} d\xi e^{\frac{i}{\hbar}p\xi} \langle q - \xi/2 | e^{-\beta\hat{H}} | q + \xi/2 \rangle, \quad (2)$$

where $\beta = \frac{1}{kT}$ is the value inversely proportional to temperature, \hat{H} is the Hamilton operator obtained from (1) by replacing p , q on the momentum and the coordinates operators \hat{p} , \hat{q} respectively. The Wigner function $W(p, q)$ can be formally considered as a generalization of the classical distribution function in phase space to quantum mechanical systems. At the same time, this generalization should not be taken literally, because, although the Wigner function is real, it can take both positive and negative values.

As example, let us consider the momentum distribution function for the canonical ensemble, which can be obtained from

$$W(p) = \int_{-\infty}^{+\infty} dq \int_{-\infty}^{+\infty} d\xi e^{\frac{i}{\hbar}p\xi} \langle q - \xi/2 | e^{-\beta\hat{H}} | q + \xi/2 \rangle. \quad (3)$$

III. PATH INTEGRAL REPRESENTATION

Now we need to calculate the density matrix (the integral in (3)). In the general case, this cannot be done directly, since the kinetic and potential energy operators entering the Hamiltonian are non-commutative, and the statistical operator $\exp(-\beta\hat{H})$ does not split into the product of the operators $\exp(-\frac{\beta\hat{p}^2}{2m})$ and $\exp(-\beta U(\hat{q}))$. Therefore, we use the following procedure, leading to the representation of the density matrix in the form of a path integral. We break the statistical operator $\exp(-\beta\hat{H})$ into the product $2K$ of the same operators $\exp(-\varepsilon\hat{H})$, where $\varepsilon = \frac{\beta}{2K}$, assuming the integer K is large enough. Then between these operators we insert $2K - 1$ of the unit operators $\hat{1}$, which we respectively replace by completeness relations for states with a certain coordinate $|q\rangle$:

$$\begin{aligned} & \langle q - \xi/2 | e^{-\beta\hat{H}} | q + \xi/2 \rangle e^{-\varepsilon\hat{H}} \dots e^{-\varepsilon\hat{H}} | q + \xi/2 \rangle = \\ & = \langle q - \xi/2 | e^{-\frac{\beta}{2K}\hat{H}} \hat{1} \dots \hat{1} e^{-\frac{\beta}{2K}\hat{H}} | q + \xi/2 \rangle \\ & = \int \dots \int dq_{-K+1} \dots dq_{K-1} \left[\prod_{k=-K}^{K-1} \langle q_{k+1} | e^{-\frac{\beta}{2K}\hat{H}} | q_k \rangle \right]. \end{aligned} \quad (4)$$

For a small ε corresponding to a large K , 'high-temperature' statistical operators $\exp(-\varepsilon\hat{H})$ can be decomposed into the product of the operators $\exp(-\frac{\varepsilon\hat{p}^2}{2m})$ and $\exp(-\frac{\varepsilon}{2}U(\hat{q}))$ up to $O(\varepsilon^2)$. After that, the corresponding matrix elements can be calculated directly using the completeness relations for states with a certain momentum $|p\rangle$, plane waves $\langle q|p\rangle = \frac{i}{\hbar}pq$ and taking into account the fact that the states $|p\rangle$ and $|q\rangle$ are proper for the operators \hat{p} and \hat{q} respectively. A small parameter $\Delta\tau = \varepsilon\hbar$ has the dimension of time. We substitute the 'high-temperature' matrix elements into the formula (4) and pass from the integration variables q and ξ to the variables $q_{-K} = q + \xi/2$ and $q_{+K} = q - \xi/2$. As a result, we obtain the path integral representation of the Wigner function.

For example, the momentum distribution function can be written in the form of a multiple integral over the coordinates q_k , $k = 0, \pm 1, \dots, \pm K$:

$$W(p, q) = \left(\frac{2\pi\hbar\Delta\tau}{m} \right)^{-K} \int d\xi \int \dots \int dq_{-K+1} \dots dq_{K-1} e^{-\Phi_{2K+1}(q_{-K}, \dots, q_K)} + O(\Delta\tau), \quad (5)$$

$$\Phi_{2K+1}(q_{-K}, \dots, q_K) = -\frac{i}{\hbar} p\xi + \frac{\Delta\tau}{\hbar} \sum_{k=-K}^{K-1} \left[\frac{m}{2} \left(\frac{q_{k+1} - q_k}{\Delta\tau} \right)^2 + \frac{U(q_{k+1}) + U(q_k)}{2} \right].$$

The parameter $\Delta\tau = \frac{\beta\hbar}{2K}$ tends to zero for $K \rightarrow \infty$, while the formula becomes accurate. However calculation of the integrals like (5) is practically impossible due to the mentioned above 'sign problem' related to the strong oscillations of the complex valued integrand.

For power dependence potential field the discrete expression (5) consists of the following factors:

$$I_k = \int_{-\infty}^{+\infty} dq_k \exp \{ a_k q_k^2 + b_k q_k + c_k + d_k q_k^\alpha \} \quad (6)$$

where integration is carried out over the real axis of $q_k \in C_{\mathbb{R}}$

The integrand is also be analytic, which allow us to use the Cauchy's integral theorem and deform the integration contour on the complex plane $q_k \in \mathbb{C}$ with the constant value of the integral I_k . (Note that the analytical structure of the integrand is mainly determined by the function q^α , since the polynomial $a_k q_k^2 + b_k q_k + c_k$ is, obviously, a analytic single-valued function.) Let us stress that detailed consideration of the (6)-like integrals for nonanalytical action is presented in [18].

IV. BASICS OF THE COMPLEXIFICATION ON LEFSCHETZ THIMBLES

According to the Morse theory [1, 2, 19–22] the regions of integration over each real q_k in the path integrals (5), (6) is equivalent to the integration over complex valued set of Lefschetz thimbles which is homologically equivalent due to the Cauchy's integral theorem to the integration on real cycle $C_{\mathbb{R}}$. Assuming that q_k takes the complex values $q_k \in \mathbb{C}$ and the action $\Phi[q_k(\tau)]$ is extended to a holomorphic function of q let us consider the set Σ of critical points (saddle points) $q_{k,\sigma}$, which satisfy condition $\partial\Phi[\bar{q}]/\partial\bar{q}|_{\bar{q}=\bar{q}_{k,\sigma}} = 0$. The real Morse function in our case can be defined as $h \equiv -\Re\{\Phi[q_k]\}$ and the associate gradient (downward) flow equations is given by:

$$\frac{d\mathbf{q}}{dl} = -\frac{\partial\bar{\Phi}(\mathbf{q})}{\partial\mathbf{q}}, \quad l \in \mathbb{R}. \quad (7)$$

The Morse function h is always strictly decreasing along a flow. Associated with a critical point $q_{k,\sigma}$, a Lefschetz thimble Υ_σ [23] is defined by the union of all downward flows, which trace back to $q_{k,\sigma}$ at $l \rightarrow -\infty$. Let us note that if $q_k(l)$ equals a critical point at some l , then the flow equation implies that $q_k(l)$ is constant for all l . So a non constant flow can only reach a critical point at $l \rightarrow -\infty$.

One can also introduce another submanifold Π_τ of by the union of all upward flows, satisfying equation with opposite sign to equation (7)

$$\frac{d}{dl} \tilde{q}_k(l) = \frac{\partial\bar{\Phi}[\tilde{q}_k]}{\partial\tilde{q}_k}, \quad l \in \mathbb{R}^1 \quad (8)$$

which converge to $q_{k,\tau}$ at $l \rightarrow -\infty$, so that its intersection number with $q_k(l) \in \Upsilon_\sigma$ is unity and vanishing otherwise, $\langle \Upsilon_\sigma, \Pi_\tau \rangle = \delta_{\sigma,\tau}$.

Strictly speaking this means that $q_k(l) \in \Upsilon_\sigma$ if $q_k(l)$ is the solution of Eq. (7) and for any positive (may be very small) $\epsilon > 0$ there exists the positive (may be very large) $L > 0$ that for all negative l such that $-l > L$ we have $\|q_k(l) - q_{k,\sigma}\| < \epsilon$. This allow in numerical simulation to use the following approximation. Due to the restrictions on computational time at solving equation (7), (8) it is necessary to exclude the small ϵ vicinity of critical point, where the parameter $l \rightarrow -\infty$. So in numerical simulations the starting points for downward flow have to be chosen outside of a small vicinity of $q_{k,\sigma}$ and the averaging results of calculations by the Monte Carlo method can be done over ensemble of the downward flows related to decreasing small ϵ . Algorithm of this MC approach, sampling the main contribution in integrals like (5), (6) will be discussed below.

Then, according to Morse theory [23], it follows that

$$C_{\mathbb{R}} = \sum_{\sigma \in \Sigma} n_{\sigma} \Upsilon_{\sigma}, \quad n_{\sigma} = \langle C_{\mathbb{R}} | \Pi_{\sigma} \rangle \quad (9)$$

which holds in the homological sense. Now, for example, the momentum distribution function Eq. (3) can be given by the formula

$$W(p) = \sum_{\sigma \in \Sigma} n_{\sigma} e^{-i\Im(\Phi[q(\tau)])} \int_{\Upsilon_{\sigma}} Dq(\tau) e^{-\Re(\Phi[q(\tau)])}, \quad (10)$$

As consequence, for the critical points \mathbf{q}_{σ} satisfying $\Re[-\Phi(\mathbf{q}_{\sigma})] \geq \max \Re(-\Phi(q))$, $q \in C_{\mathbb{R}}$, it holds that $\langle C_{\mathbb{R}} | \Pi_{\sigma} \rangle = 0$ and the associated thimbles do not contribute to the path integration. On the other hand, it holds that if $\langle C_{\mathbb{R}} | \Pi_{\sigma} \rangle = 1$ the associated thimbles contribute with the relative weights proportional to $e^{-\Re(\Phi[q(\tau)])}$.

V. ALGORITHMIC SOLUTION

To do calculation, for example, the momentum distribution function $F(p)$ we are going to combine the Monte Carlo method (MC) [24, 25] for searching the critical points q_{σ} and the finite-difference methods for solving equations (7), (8) with initial conditions obtained by MC method in the small ϵ vicinity of \bar{q}_{σ} . In this section we will be a little bit sloppy in our notation as the symbol $\bar{\mathbf{q}}$ can denote a complex valued $(2K - 1)$ -dimensional variables.

Used here MC method is based on the Metropolis – Hastings algorithm [24, 25], which resides in designing a Markov process (by constructing transition probabilities $P(\bar{\mathbf{q}} \rightarrow \bar{\mathbf{q}}')$), such that its stationary distribution to be equal to $w(\bar{\mathbf{q}})$. The derivation of the algorithm starts with the condition of detailed balance:

$$w(\bar{\mathbf{q}})P(\bar{\mathbf{q}} \rightarrow \bar{\mathbf{q}}') = w(\bar{\mathbf{q}}')P(\bar{\mathbf{q}}' \rightarrow \bar{\mathbf{q}}) \quad (11)$$

which can be rewritten as

$$\frac{P(\bar{\mathbf{q}} \rightarrow \bar{\mathbf{q}}')}{P(\bar{\mathbf{q}}' \rightarrow \bar{\mathbf{q}})} = \frac{w(\bar{\mathbf{q}}')}{w(\bar{\mathbf{q}})}. \quad (12)$$

To increase efficiency of the numerical procedure we are going to separate the transition in two sub-steps: the proposal and the acceptance-rejection. The transition probability can be written as the product: $P(\bar{\mathbf{q}} \rightarrow \bar{\mathbf{q}}') = g(\bar{\mathbf{q}} \rightarrow \bar{\mathbf{q}}')A(\bar{\mathbf{q}} \rightarrow \bar{\mathbf{q}}')$. The proposal distribution $g(\bar{\mathbf{q}} \rightarrow \bar{\mathbf{q}}')$ is the conditional probability of proposing a state $\bar{\mathbf{q}}'$ for given $\bar{\mathbf{q}}$. The acceptance distribution $A(\bar{\mathbf{q}} \rightarrow \bar{\mathbf{q}}')$ is the conditional probability to accept the proposed state $\bar{\mathbf{q}}'$.

Inserting this relation in the previous equation, we have

$$\frac{A(\bar{\mathbf{q}} \rightarrow \bar{\mathbf{q}}')}{A(\bar{\mathbf{q}}' \rightarrow \bar{\mathbf{q}})} = \frac{w(\bar{\mathbf{q}}')}{w(\bar{\mathbf{q}})} \frac{g(\bar{\mathbf{q}}' \rightarrow \bar{\mathbf{q}})}{g(\bar{\mathbf{q}} \rightarrow \bar{\mathbf{q}}')}. \quad (13)$$

Then it is necessary to choose an acceptance that fulfills detailed balance. One common choice is the Metropolis's suggestion:

$$A(\bar{\mathbf{q}} \rightarrow \bar{\mathbf{q}}') = \min \left(1, \frac{w(\bar{\mathbf{q}}')}{w(\bar{\mathbf{q}})} \frac{g(\bar{\mathbf{q}}' \rightarrow \bar{\mathbf{q}})}{g(\bar{\mathbf{q}} \rightarrow \bar{\mathbf{q}}')} \right). \quad (14)$$

This means that we always accept when the acceptance is bigger than 1 and we can accept or reject when the acceptance is smaller than 1.

To optimize the MC search of the critical point $\partial \bar{\Phi}[\bar{q}]/\partial \bar{q}|_{\bar{q}=\bar{q}_{k,\sigma}} = 0$ we define the probability $w(\bar{\mathbf{q}})$ as $w(\bar{\mathbf{q}}) = \exp(-b|\partial \bar{\Phi}[\bar{\mathbf{q}}]/\partial \bar{\mathbf{q}}|^2)$ with parameter $b \geq 1$. We are free in choosing probability $g(\bar{\mathbf{q}} \rightarrow \bar{\mathbf{q}}')$ as it affect only the efficiency of sampling the main contribution to the integrals and does not change the final result of calculations. For optimization of the MC finding the main contribution to the integral (10) the choice of the $g(\bar{\mathbf{q}} \rightarrow \bar{\mathbf{q}}')$ may be the following $g(\bar{\mathbf{q}} \rightarrow \bar{\mathbf{q}}') = e^{-\beta \Re(\Phi[\bar{\mathbf{q}}'])}/e^{-\beta \Re(\Phi[\bar{\mathbf{q}}])}$ with free appropriate fit parameter β .

The Metropolis – Hastings algorithm consists in the following steps:

1. Initialization: pick an initial state point $\bar{\mathbf{q}}$ at random.

2. Randomly pick a state $\bar{\mathbf{q}}'$, according to probability $g(\bar{\mathbf{q}} \rightarrow \bar{\mathbf{q}}')$.
3. Accept the state according to the probability $A(\bar{\mathbf{q}} \rightarrow \bar{\mathbf{q}}')$. If not accepted, that means that $\bar{\mathbf{q}}' = \bar{\mathbf{q}}$, and so there is no need to update anything. Else, the system transits to $\bar{\mathbf{q}}'$.
4. Go to 2 until many M states were generated to "forget" initial $\bar{\mathbf{q}}$ and to obtain the average position of the critical point $\langle \bar{\mathbf{q}} \rangle$.
5. If $w(\langle \bar{\mathbf{q}} \rangle) \geq 0.95$ carry out several iterations by complex-valued extension of the Newton's method to produce better approximations to the roots (or zeroes) of the complex-valued function $\partial \bar{\Phi}[\bar{q}]/\partial \bar{q}|_{\bar{q}=\bar{q}_\sigma} = 0$. Else go to 2.
6. Save the state $\bar{q}_\sigma = \langle \bar{\mathbf{q}} \rangle$.
7. At random pick an initial point $\bar{\delta \mathbf{q}}$ at the small vicinity of the zero point of the complex space (may be in any given quarter).
8. Analogously randomly pick a new state $\bar{\delta \mathbf{q}}'$ according to the probability $g(\bar{\mathbf{q}}_\sigma + \delta \mathbf{q} \rightarrow \bar{\mathbf{q}}_\sigma + \delta \mathbf{q}')$.
9. Go to 8 many times M' to "forget" initial $\bar{\delta \mathbf{q}}$ state and to obtain the average value of the $\langle \bar{\delta \mathbf{q}}' \rangle$.
10. Solve equation (8) with initial conditions of $\bar{\mathbf{q}}_\sigma + \langle \delta \mathbf{q}' \rangle$ to check if $n_\sigma = \langle C_{\mathbb{R}}, \Pi_\sigma \rangle = 1$. If $n_\sigma = 1$ go to 11, otherwise go to 2.
11. Solve equation (7) with initial conditions of $\bar{\mathbf{q}}_\sigma + \langle \delta \mathbf{q}' \rangle$ until modulus of the integrand in (10) will be smaller of several order of magnitude of its initial value and calculate the integral sum related to (10).
12. Go to 2 many times and calculate the integrals (10).

It is important to notice that it is not clear, in a general problem, which distribution $g(\bar{\mathbf{q}} \rightarrow \bar{\mathbf{q}}')$ one should use. It is a free parameter of the method which has to be adjusted to the particular problem 'in hand'. This is usually done by calculating the acceptance rate, which is the fraction of proposed samples that is accepted during the last N samples. As has been shown theoretically the ideal acceptance rate have to be in interval of 23 – 50 %.

VI. RESULTS OF NUMERICAL TEST CALCULATIONS

Before calculation of the Fourier transform defining the Wigner function (2) it is necessary to test the proposed algorithm by calculation of the more simple contour integrals with know analytical or numerical answer. We started from consideration of the strongly oscillating and low dimensional integrals, which can be typically treated very effectively with the saddle point integration method. Presented test calculations provide an interesting benchmark for more realistic path integrals. It is also non-trivial from the point of view of a Monte Carlo integration.

A. The Airy function

Let us consider a classic example: the Airy function is defined as the integral over the real axis $C_{\mathbb{R}}$:

$$\text{Ai}(p) = \frac{1}{2\pi} \int_{-\infty}^{+\infty} dx \exp \left[i \left(px + \frac{x^3}{3} \right) \right], \quad (15)$$

The integrand is strongly oscillating function on $C_{\mathbb{R}}$, which makes a direct numerical evaluation infeasible. The left plot of the Fig. 1 shows lines of the constant imaginary part of the power in exponent in (15) on complex plane, while increasing and lowering values are denoted by the red and blue regions. The critical points are in the left upper and the right bottom quarters of the complex plane. We can deform the integration path in the complex plane of variable $z = x + iy$, as long as the new path belongs to the original relative homology class, which connects regions of strongly decaying modulus of the integrand at infinity (blue regions on the centre plot of the Fig. 1). Right panel of this figure shows the contour plot of the MC probability $w(\bar{\mathbf{q}}) = \exp(-b|\partial \bar{\Phi}[\bar{\mathbf{q}}]/\partial \bar{\mathbf{q}}|^2)$ with two red circles at its maximum values at the critical points.

Testing the proposed approach starts from finding critical points by suggested MC method. It turns out that the Markovian chain traveling on the whole complex plane always stabilizes in the vicinity of the the critical point $z_\sigma = -1.11 + i1.79$ (point in the left upper quarter of the complex plane in Fig. 1) ignoring the second critical point

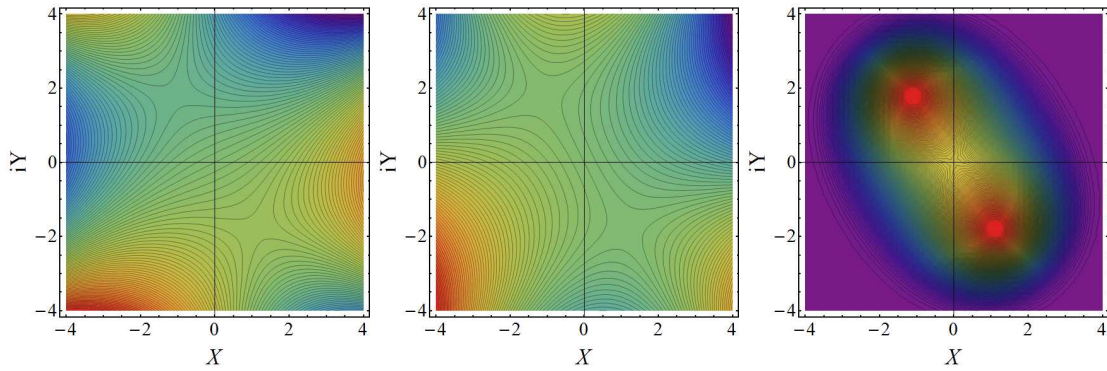


Figure 1: (Color online) The contour plot of the imaginary part (left panel) and the real part (central panel) of the power in exponent in (15) on complex plane for $p = 2 + 4i$. (Right plot) Contour plot of the probability $w(\bar{q}) = \exp(-b|\partial\bar{\Phi}[\bar{q}]/\partial\bar{q}|^2)$.

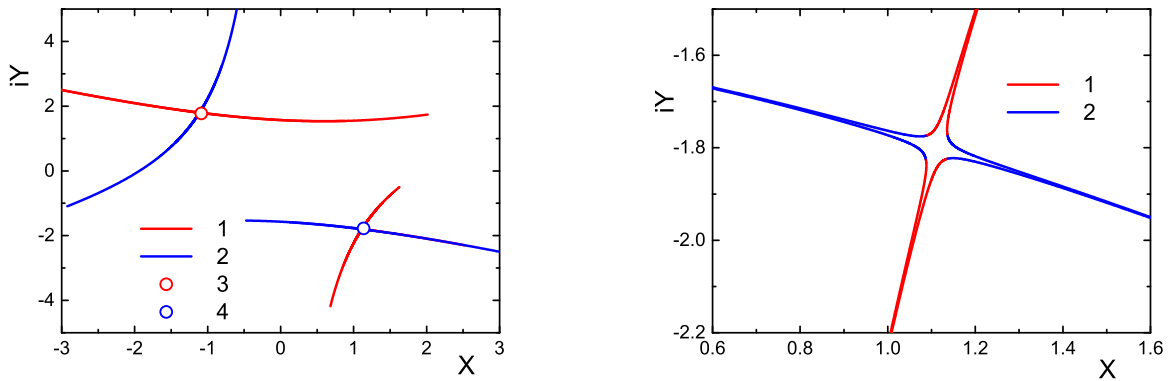


Figure 2: (Color online) (Left plot) The averaged downward flows are lines $-1 (\in \Upsilon_\sigma)$ and the upward flows are lines $-2 (\in \Pi_\sigma)$. The critical points are points 3 and 4 ($\partial\bar{\Phi}[\bar{q}]/\partial\bar{q} = 0$) of the integrand in (15). Red critical point and the associated thimbles contribute to the contour integral of the Airy function (15) as $\langle C_{\mathbb{R}}, \Pi_\sigma \rangle = 1$, while the blue point not, as $\langle C_{\mathbb{R}}, \Pi_\sigma \rangle = 0$. (Right plot) Details of initial conditions obtained by MC method in different quarters of small vicinity of the critical point.

($z_\sigma = +1.11 - i1.79$) in the favoure of the the first one. So to force the Markovian chain to stabilize in the vicinity of the second critical point we have to use the special restrictions. Reason of this behavior of the Markovian chain is the asymmetry of the contour plots of the real and imaginary parts of the power in exponent in (15) (see the Fig. 1).

Solution of the complex valued differential equations (7 and 8) with MC initial conditions nearby the both critical points allow to obtain averaged downward (red lines) and upward (blue lines) flows (see both plots of the Fig. 2). Right plot of this figure shows in details the downward and upward flows from different quarters of the small enough vicinities of the critical points. Let us note that initial conditions for red downward and blue upward flows were the same to test their fast converge to the related Υ_σ and Π_σ respectively. Let us note that the power low grows on the complex plane of the right part of differential equations (7) and (8) results in limitations on the 'time' l of obtained solutions at needed given accuracy.

Table I: The MC results versus the exact Airy function

p	MC	$theAiryfunction$
$2+i4$	$0.3365 - i0.065451$	$0.3301 - i0.088$
$0+i4$	$-4.8569 + i7.244$	$-4.6362 + i7.4111$
$4+i0$	$0.000738 + i0.00006$	$0.000952 + i0$

As only the blue line for red point crosses the real axis ($\langle C_{\mathbb{R}}|\Pi_\sigma \rangle = 1$) we calculate integral defined the Airy function along the red Lefschetz thimble. As we mentioned above the Markovian chain traveling on the whole

complex plane prefer namely this critical point ignoring the second one. The reason of this interesting fact has been further investigated.

Result of calculation at $p = 2 + i4$ is presented in Table 1 as well as results of the some additional calculations for $p = 0 + i4$ and $p = 4 + i0$. Comparison of obtained results with well known values of Airy function demonstrate a good enough agreement. Discrepancy between exact values of the Airy function and related values obtained by proposed procedure can be explained by approximations used in transitions from initial integral to its Lefschetz thimbles representation accounting for only the main contribution to the contour integrals.

B. Short time path integral

Now to test the developed approach let us consider elementary factor (6) in the finite dimensional approximation of the path integral. Expression (6) may be rewritten in the form like:

$$I_k(p_k) = \int_{-\infty}^{+\infty} dq_k \exp \{ i(p_k q_k + i((q_k - \text{const})^2 + q_k^4/4)) \}, \quad (16)$$

where, for example, $\text{const} = 2$.

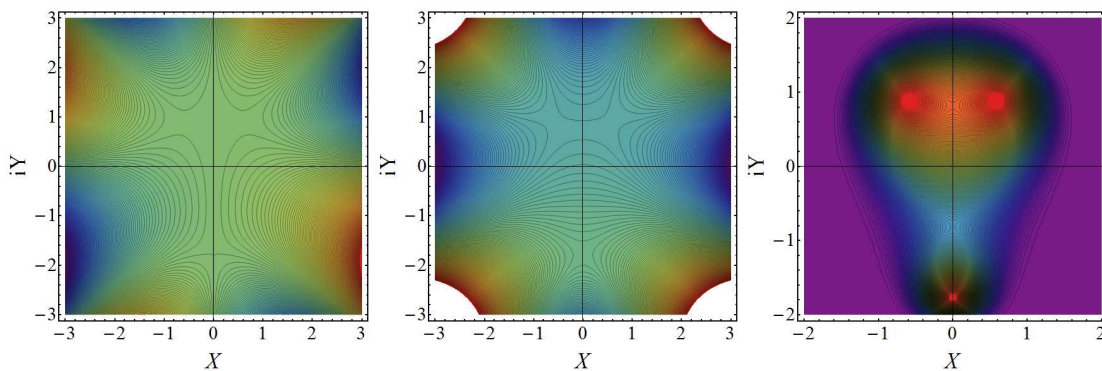


Figure 3: (Color online) The contour plot of imaginary part (left panel) and real part (central panel) of the power in exponent in (16) on complex plane for $\text{const} = 2$. (Right plot) Contour plot of the probability $w(\bar{\mathbf{q}}) = \exp(-b|\partial\bar{\Phi}[\bar{\mathbf{q}}]/\partial\bar{\mathbf{q}}|^2)$.

The left and right plots of Fig. 3 are the contour plots of the image and real parts of the power of exponent in integrand in (16) respectively. Right plot of the Fig. 3 presents contour plot of the probability, $w(\bar{\mathbf{q}}) = \exp(-b|\partial\bar{\Phi}[\bar{\mathbf{q}}]/\partial\bar{\mathbf{q}}|^2)$ which with conditional probability $g(\bar{\mathbf{q}} \rightarrow \bar{\mathbf{q}}')$ allows to find by MC method the critical points and provides the initial conditions for solution of the equations (7) and (8). According to the Monte Carlo simulation the critical points are $z_1 \approx 0.5712 + i0.8786$, $z_2 \approx -0.5712 + i0.8786$ and $z_3 \approx -1.77 + i0.0$, which agree with the regions of the saddle-like behaviour of the contour lines on left and right plots of Fig. 3. Here the Markovian chain traveling on the whole complex plane always stabilizes in the vicinity of the the critical point z_1 and z_2 ignoring the point z_3 .

As before solution of the complex valued differential equations (7) and (8) with MC initial conditions nearby the both upper critical points allow to obtain averaged downward (red lines) and upward (blue lines) flows (see Fig. 4). As the both blue lines for red point cross the real axis ($\langle C_{\mathbb{R}}|\Pi_{\sigma} \rangle = 1$) we calculate sum of the contributions to the integral (16) along the both red Lefschetz thimbles with opposite sign due to the different thimble orientation. According to the Morse theory contribution of the bottom critical point has to be ignored as the related blue line does not cross real axis (here not shown) and the maximum of the integrand on the real axis is smaller than the value of the integrand at this critical point.

As before details the MC initial conditions and related downward and upward flows are presented by right plot of the Fig. 4. Let us note that red and blue lines start at the same MC initial points. Reason of asymmetry in behavior of the red and blue lines is in asymmetry of the real and imaginary parts of the power in exponent. (see the Fig. 4). Let us stress the fast convergence of the upward and downward flows to the related limit lines Υ_{σ} and Π_{σ} . Comparison of the Monte Carlo result for $I_k = 0.01306 + i0.00006$ with independent exact calculations $I_k = 0.01402 + i0$ demonstrate a good enough accuracy of the developed approach.

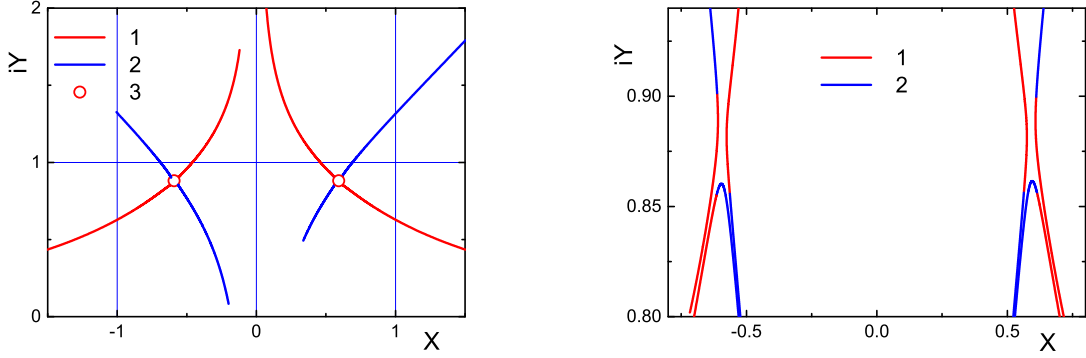


Figure 4: (Color online) The averaged downward flows are lines - 1 ($\in \Upsilon_\sigma$) and the upward flows are lines - 2 ($\in \Pi_\sigma$) at $const = 2$ and $p = 2 + i4$. The critical points of the integrand in (16) are points 3 ($\partial\bar{\Phi}[\bar{q}]/\partial\bar{q} = 0$). Red critical point and the associated thimbles contribute to the contour integral (16) as $\langle C_{\mathbb{R}}, \Pi_\sigma \rangle = 1$. (Right plot) Details of MC initial conditions in different quarters of small vicinity of the critical points.

VII. 'THE SIGN PROBLEM' OF THE REAL VALUED PATH INTEGRALS.

The second type of the 'sign problem' discussed in Introduction arises from requirement of antisymmetrization of the real valued matrix elements of the density matrix to account for Fermi statistical effects. In this section to avoid this type of 'sign problem' we are going to discuss the effective pair pseudopotential in phase space, which realizes the Pauli blocking of fermions due to the repulsion between identical fermions preventing their occupation of the same phase space cell. In this approximation the pseudopotential is used instead of antisymmetrization of matrix elements.

The antisymmetrized Wigner function of many-particle electron - hole system in canonical ensemble can be defined as a Fourier transform [26, 27] of the matrix element of the density operator [28] in the coordinate representation:

$$\begin{aligned}
W(p, x) &= \sum_{\sigma, \sigma'} \int d\xi \delta_{\sigma, \sigma'} \exp(i\langle \xi | p \rangle) \langle x + \xi/2, \sigma | e^{-\beta \hat{H}} | x - \xi/2, \sigma' \rangle \\
&= \frac{C(M)}{Z(N_{eh}, V, \beta)} \sum_{\sigma} \sum_{P_e P_h} (-1)^{\kappa_{P_e} + \kappa_{P_h}} \mathcal{S}(\sigma, P_{eh}; \sigma') \Big|_{\sigma' = \sigma} \\
&\times \int d\xi \int dq^{(1)} \dots dq^{(M-1)} \exp \left\{ -\pi \frac{\langle \xi | P_{eh} + E | \xi \rangle}{2M} + i\langle \xi | p \rangle - \pi \frac{|P_{eh}x - x|^2}{M} \right. \\
&\left. - \sum_{m=0}^{M-1} \left[\pi |q^{(m)} - q^{(m+1)}|^2 + \varepsilon U \left((P_{eh}x - x) \frac{m}{M} + x + q^{(m)} - \frac{(M-m)\xi}{2M} + \frac{mP_{eh}\xi}{2M} \right) \right] \right\},
\end{aligned} \tag{17}$$

where $C(M)$ is constant and the multidimensional vectors p q σ present all momenta, coordinates and spin variables of particles. The antisymmetrization for electrons and holes takes into account the Fermi statistics. Here in the sum over all permutations $P_e P_h$ we have replaced variables of integration $x^{(m)}$ for any given permutation $P_e P_h$ by relation

$$x^{(m)} = (P_{eh}x - x) \frac{m}{M} + x + q^{(m)} - \frac{(M-m)\xi}{2M} + \frac{mP_{eh}\xi}{2M}. \tag{18}$$

where $q^{(M)} = q^{(0)}$. Details of deriving the Wigner function (17) are presented in [11, 28–34].

As it was shown in [35] due to the Fermi repulsion of fermions the main contribution to Fermi statistics in (17) comes from the pair permutations even at temperatures less the Fermi energy. This is the physical reason to take into account only identical and pair permutations and neglect the others.

To avoid difficulties at Monte Carlo simulations due to arising the delta-function after the Fourier transform the positive Husimi distributions, being a coarse-grained Wigner function, can be used with a Gaussian smoothing for small phase space cells of parameters Δ_x^2 and Δ_p^2 [27]. The final expression for Wigner function can be written in the form:

$$\begin{aligned}
W^H(p, q,) &\approx \frac{C(M)}{Z(N_{eh}, V, \beta)} \int dq^{(1)} \dots dq^{(M-1)} \\
&\times \exp \left\{ - \sum_{m=0}^{M-1} \left[\pi |q^{(m)} - q^{(m+1)}|^2 + \varepsilon U(q + q^{(m)}) \right] \right\} \\
&\times \exp \left\{ \frac{M}{4\pi} \left| ip + \frac{\varepsilon}{2} \sum_{m=0}^{M-1} \frac{(M-2m)}{M} \frac{\partial U(q + q^{(m)})}{\partial x} \right|^2 \right\} \\
&\times \sum_{\sigma} \exp(-\beta \sum_{l < t}^{N_e} v_{lt}^e) \exp(-\beta \sum_{l < t}^{N_h} v_{lt}^h)
\end{aligned} \tag{19}$$

where the effective phase space pair pseudopotentials, accounting for quantum statistical effects in pair approximation, look like:

$$\begin{aligned}
v_{lt}^a &= -kT \ln \left\{ 1 - \delta_{\sigma_{l,a} \sigma_{t,a}} \exp \left(- \frac{2\pi |q_{l,a} - q_{t,a}|^2 \left(1 - \frac{\tilde{\Delta}_{a,x}^2 / \lambda_a^2}{1 + \tilde{\Delta}_{a,x}^2 / \lambda_a^2} \right)}{\lambda_a^2} \right) \exp \left(- \frac{|(\tilde{p}_{l,a} - \tilde{p}_{t,a})|^2 \lambda_a^2}{(2\pi\hbar)^2 (\tilde{\Delta}_p^2 / \lambda_a^2)} \right) \right\} \\
\tilde{p}_{t,a} &= p_{t,a} + \frac{\varepsilon}{2} \sum_{m=0}^{M-1} \frac{\partial U(q + q^{(m)})}{\partial q_{t,a}}.
\end{aligned}$$

Here $a = e, h$, $\Delta_{a,x}^2 = \frac{2}{(\pi^2 - 2)}$ and $z = 1/\sqrt{2}$, the interaction energy U is the sum of the two-particle quantum Kelbg – Coulomb pseudopotentials, the $\delta_{\sigma, \sigma'}$ are the Kronecker symbols. The phase space pseudopotentials v_{lt}^a allow us to avoid the famous 'fermionic sign problem' and to realize the Pauli blocking for electrons/holes with the same spin without antisymmetrization. Note also that the expression (19) explicitly contains the term, related to the classical Maxwell distribution, modified by terms accounting for influence of interaction on the momentum distribution function. To extent the region of applicability of obtained phase space pair pseudopotential, $\tilde{\Delta}_p^2$ and $\tilde{\Delta}_Q^2$ can be considered as fit functions with values much smaller than unity. Our test calculations [35] have shown that the best fit for $\tilde{\Delta}_p^2$ can be written in the form $\tilde{\Delta}_p^2 / \lambda_a^2 = 0.00505 + 0.056n\lambda_a^3$, while $\tilde{\Delta}_{a,x}^2$ and $\tilde{\Delta}_Q^2$ were of order 0.1.

Figure 5 presents contour panels of effective pair pseudopotentials for parameter of degeneracy $n\lambda_e^3$ equal to 5.6 ($T/E_F = 0.208$). Momenta and coordinates axes are scaled by the electron thermal wave length with Plank constant and factor ten for momentum.

For ideal ($U \equiv 0$ in 19) electron–hole plasma the Figure 5 shows the momentum distributions $W_a(|p_a|)$, ($a = e, h$) scaled by ratio of the Plank constant to the electron thermal (de Broglie) wavelength ($\frac{\hbar}{\lambda_e}$). In the Figure 5 results of Monte Carlo calculations for electrons and holes are presented by lines 1 and 3, while lines 2 and 4 shows ideal Fermi distributions. Presented distribution functions are normalized to one. Note that, in these calculations, holes are twice as massive as electrons, so the corresponding degeneracy parameters are $2^{3/2}$ times smaller. It follows from the analysis of Figure 5 that the agreement between the MC calculations and the analytical Fermi distributions are good enough up to a value of the electron degeneracy parameter equal to $n\lambda_e^3 \approx 6$ where decay of the distribution functions is about of five orders of magnitude.

So the Pauli blocking in phase space accounted for by these exchange pseudopotentials provides agreement of MC calculations and analytical Fermi distribution in wide ranges of fermion degeneracy and fermion momenta, where decay of the distribution functions is at least of five orders of magnitude. It necessary to stress that one of the reason of increasing discrepancy with degeneracy growth is limitation on available computing power allowing calculations with several hundred particles each presented by twenty beads. When parameter of degeneracy is more than 10 ($T/E_F = 0.141$) the thermal electron wave length is of order of Monte Carlo cell size and influence of finite number of particles and periodic boundary conditions becomes significant.

Let us stress that detailed test calculation for interacting particle carried out within developed approach in [30, 31] have demonstrated good agreement with results of independent calculations by standard path integral Monte Carlo method and available analytical results.

VIII. CONCLUSION

One of the main difficulty for the Path Integral Monte Carli simulation of the quantum systems of particles is so called 'sign problem'. However nowadays the term 'sign problem' is used to identify two different problems.

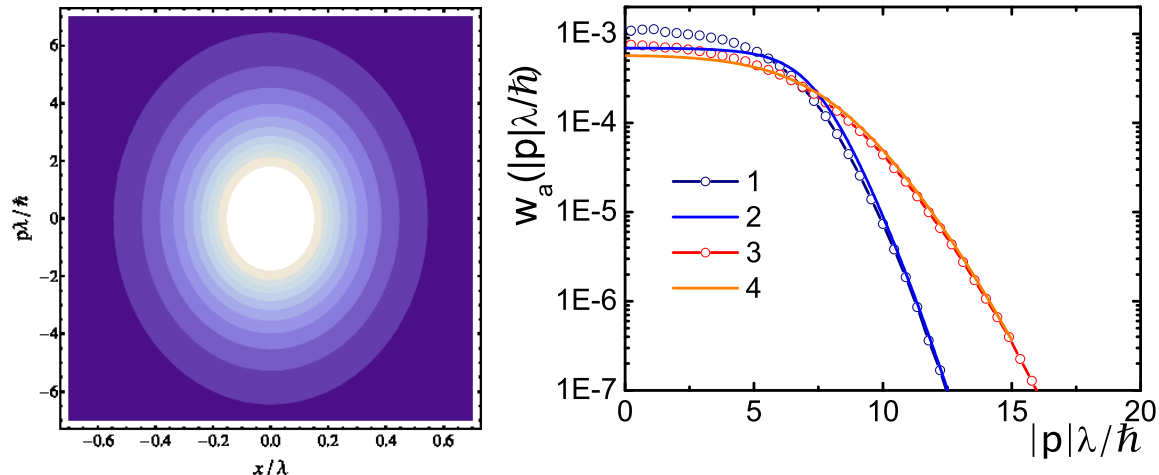


Figure 5: (Color online)(Left panel) Contour plots of the repulsive effective exchange pair pseudopotentials in phase space. Dark area $\beta v_{it}^e \approx 0$, white area $\beta v_{it}^e \geq 1.9$. (Right panel) The momentum distribution functions $W_a(|p|)$ for ideal electrons ($a=e$) and two times heavier holes ($a=h$). Lines: 1, 3 – MC distributions $W_a(|p|)$ scaled by ratio of Planck constant to the electron thermal (de Broglie) wavelength ($\frac{\hbar}{\lambda_e}$), while lines 2, 4 demonstrate the analytical Fermi distributions. Parameters of degeneracy $n\lambda_e^3$ for electrons is $n\lambda_e^3 = 5.6$ ($T/E_F = 0.208$, $k_F\lambda_e = 5.5$).

The ideas to overcome the first type of the ‘sign problem’ of strongly oscillating complex valued integrand in the Feynman path integrals comes from Picard-Lefschetz theory and a complex version of Morse theory. The main idea is to select Lefschetz thimbles as the cycle approaching the saddle point at the path-integration, where the imaginary part of the complex action stays constant. Since the imaginary part of the action is constant on each thimble, the sign problem disappears and the integral can be calculated much more effectively. In this work some simple test calculation and comparison with available analytical results have been carried out. We hope that the presented simple testing is a perfect playground to see thimble regularization at work. It is instructive both for inspecting the structure of relevant thimbles and from the algorithmic point of view.

The second type of the ‘sign problem’ arises at studies the Fermi systems by path integral approach and is caused by the requirement of antisymmetrization of the real valued matrix elements of the density matrix. To overcome this issue the new numerical version of the Wigner approach to quantum mechanics for treatment thermodynamic properties of degenerate systems of fermions has been developed. Here the main idea is to derived pseudopotential in phase space depending on the coordinates and momenta, which due to the repulsion between identical fermions prevents their occupation of the same phase space cell and so realizes the Pauli blocking. To test the developed approach calculations of the momentum distribution function of the degenerate ideal system of Fermi particles has been presented in a good agreement with analytical Fermi distributions.

IX. ACKNOWLEDGEMENTS

We acknowledge stimulating discussions with Profs. Yu.B. Ivanov.

-
- [1] M. V. Fedoryuk, in *Doklady Akademii Nauk* (Russian Academy of Sciences, 1976), vol. 227, pp. 580–583.
 - [2] E. Witten, *AMS/IP Stud. Adv. Math* **50**, 347 (2011).
 - [3] A. Alexandru, G. Başar, and P. Bedaque, *Physical Review D* **93**, 014504 (2016).
 - [4] A. Alexandru, G. Başar, P. F. Bedaque, and G. Ridgway, *Physical Review D* **95**, 114501 (2017).
 - [5] G. Parisi, J. Klauder, W. Petersen, J. Ambjorn, S. Yang, F. Karsch, and H. Wyld, *Stochastic Quantization* **131**, 381 (1988).
 - [6] J. R. Klauder, *Journal of Physics A: Mathematical and General* **16**, L317 (1983).
 - [7] J. R. Klauder, *Physical Review A* **29**, 2036 (1984).
 - [8] H. Fujii, D. Honda, M. Kato, Y. Kikukawa, S. Komatsu, and T. Sano, *Journal of High Energy Physics* **2013**, 147 (2013).

- [9] A. Mukherjee, M. Cristoforetti, and L. Scorzato, *Physical Review D* **88**, 051502 (2013).
- [10] F. Di Renzo and G. Eruzzi, *Physical Review D* **92**, 085030 (2015).
- [11] W. Ebeling, V. Fortov, and V. Filinov, *Quantum Statistics of Dense Gases and Nonideal Plasmas* (Springer, Berlin, 2017).
- [12] T. Dornheim, S. Groth, A. Filinov, and M. Bonitz, *New J. Phys.* **17**, 073017 (2015).
- [13] T. Dornheim, S. Groth, T. Sjostrom, F. D. Malone, W. M. C. Foulkes, and B. M, *Phys. Rev. Lett.* **117**, 156403 (2016).
- [14] T. Schoof, M. Bonitz, A. Filinov, D. Hochstuhl, and J. W. Dufty, *Contrib. Plasma Phys.* **51**, 687 (2011).
- [15] T. Schoof, S. Groth, J. Vorberger, and M. Bonitz, *Phys. Rev. Lett.* **115**, 130402 (2015).
- [16] A. Larkin, V. Filinov, and V. Fortov, *Contributions to Plasma Physics* **57**, 506 (2017).
- [17] A. Larkin, V. Filinov, and V. Fortov, *Journal of Physics A: Mathematical and Theoretical* **51**, 035002 (2017).
- [18] M. Fedoryuk, in *Analysis I* (Springer, 1989), pp. 83–191.
- [19] V. I. Arnold, S. M. Gusein-Zade, and A. N. Varchenko, *Singularities of Differentiable Maps: Monodromy and Asymptotics of Integrals* (Birkhäuser, 1988).
- [20] F. Pham, in *Proc. Symp. Pure Math.* (1983), vol. 40, pp. 310–333.
- [21] M. Berry and C. Howls, *Proceedings of the Royal Society of London. Series A: Mathematical and Physical Sciences* **430**, 653 (1990).
- [22] C. Howls, *Proceedings of the Royal Society of London. Series A: Mathematical, Physical and Engineering Sciences* **453**, 2271 (1997).
- [23] M. Cristoforetti, F. Di Renzo, L. Scorzato, A. Collaboration, et al., *Physical Review D* **86**, 074506 (2012).
- [24] A. W. Rosenbluth, M. N. Rosenbluth, A. H. Teller, and E. Teller, *J. Chem. Phys.* **21**, 1087 (1953).
- [25] W. K. Hasting, *Biometrika* **57**, 97 (2007).
- [26] E. P. Wigner, *Phys. Rev* **40**, 749 (1932).
- [27] V. Tatarskii, *Sov. Phys. Uspekhi* **26**, 311 (1983).
- [28] V. Filinov, Y. Ivanov, M. Bonitz, V. Fortov, and P. R. Levashov, *Phys. Rev. C* **87**, 035207 (2013).
- [29] R. P. Feynman and A. R. Hibbs, *Quantum Mechanics and Path Integrals* (McGraw-Hill, New York, 1965).
- [30] A. Larkin, V. Filinov, and V. Fortov, *Contrib. Plasma Phys.* **56**, 187 (2016).
- [31] A. Larkin and V. Filinov, *Journal of Applied Mathematics and Physics* **5**, 392 (2017).
- [32] N. Wiener, *J. Math. Phys.* **2**, 131 (1923).
- [33] V. M. Zamalin and G. E. Norman, *USSR Comp. Math. and Math. Phys.* **13**, 169 (1973).
- [34] V. M. Zamalin, G. E. Norman, and V. S. Filinov, *The Monte-Carlo Method in Statistical Thermodynamics* (Nauka, Moscow, 1977).
- [35] A. S. Larkin, V. S. Filinov, and V. E. Fortov, *J. Phys. A: Math. Theor.* **51**, 035002 (2018).